# ELECTRONIC SUPPLEMENTARY INFORMATION

# Single-Molecule Microfluidic Assay for Prostate-Specific Antigen Based on Magnetic Beads and Upconversion Nanoparticles

Dorota Sklenárová,[a,#] Antonín Hlaváček,[b,#,*] Jana Křivánková,[b] Julian C. Brandmeier,[a,c] Julie Weisová,[b] Michal Řiháček,[d] Hans H. Gorris,[a] Petr Skládal,[a] and Zdeněk Farka[a,*]

*a* *Department of Biochemistry, Faculty of Science, Masaryk University, Kamenice 5, 625 00 Brno, Czech Republic*

*b* *Institute of Analytical Chemistry of the Czech Academy of Sciences, Veveří 97, 602 00 Brno, Czech Republic*

*c* *Institute of Analytical Chemistry, Chemo- and Biosensors, University of Regensburg, Universitätsstraße 31, 93053 Regensburg, Germany*

*d* *Department of Laboratory Methods, Faculty of Medicine, Masaryk University, Kamenice 5, 625 00 Brno, Czech Republic*

[#] *The authors contributed equally.*

* *Corresponding author. E-mail: hlavacek@iach.cz (A.H.), farka@mail.muni (Z.F.)*

## Table of contents

# 1 Materials and methods

## 1.1 Synthesis of UCNPs and ligand exchange reaction

The UCNPs were synthesized by high-temperature coprecipitation according to our previously published work.[1,2] The synthesis of the alkyne-PEG-neridronate linker and the preparation of azide-modified streptavidin and antibody were done in accordance with our previous publications.[3–5]

The ligand exchange reaction to remove oleic acid from the UCNP surface and introduce the click-reactive alkyne-PEG-neridronate linker was carried out as follows. UCNPs (10 mg) dispersed in cyclohexane were mixed with an equal volume of 200 mM HCl, incubated for 30 min at 38 °C under shaking, and sonicated for 15 min at room temperature to mediate phase transfer from cyclohexane to water. The upper organic phase was discarded, and a 2-fold volume excess of acetone was added to precipitate bare UCNPs. The sample was then centrifuged at 1000 *g* for 20 min, and all the solvent was discarded. The resulting UCNP pellet was redispersed in 500 µL of deionized water and sonicated for 5 min. Then, 500 µL of the alkyne-PEG-neridronate linker (4 mg/mL) in deionized water was added to the sample, followed by shaking at 38 °C overnight. To remove the non-bound linker, the sample was dialyzed in a Float-A-Lyzer G2 dialysis device with a molecular weight cut-off (MWCO) of 100 kDa (Fisher Scientific, USA) for 72 h at 4 °C against 4 L of deionized water with 1 mM KF. The dialysis medium was exchanged 9 times.

## 1.2 Preparation of UCNP-PEG-streptavidin (UCNP-SA) labels

The functionalization of UCNPs with streptavidin was carried out using a copper-catalyzed click reaction. An aqueous solution of $CuSO_4$ and THPTA (25 mM and 125 mM, respectively, 10 µL) and Tris-HCl (375 mM, pH 7.5, 100 µL) were added to 10 mg of UCNPs modified with alkyne-PEG-neridronate in deionized water with 1 mM KF (1.4 mL). Afterward, the mixture was purged for 45 min with argon, and streptavidin-azide (1 mg/mL, 100 µL) together with sodium ascorbate (100 mM, 20 µL) were added to initiate the click reaction. The dispersion was purged for another 50 min with argon. To remove the non-bound streptavidin-azide, the sample was dialyzed in a Float-A-Lyzer G2 dialysis device (100 kDa MWCO) for 72 h against 4 L of dialysis buffer (50 mM Tris, 0.05% $NaN_3$, 1 mM KF, pH 7.5) at 4 °C; the buffer was exchanged 9 times. The prepared bioconjugate was stored at 4 °C until further use.

## 1.3 Preparation of UCNP-PEG-antibody (UCNP-Ab) labels

The functionalization of UCNPs with anti-PSA polyclonal antibody (AF1344) was also done using copper-catalyzed click reaction. An aqueous solution of $CuSO_4$ and THPTA (25 mM and 125 mM, respectively, 5 µL), Tris-HCl (375 mM, pH 7.5, 50 µL), and azide-modified anti-PSA polyclonal antibody (1 mg/mL, 50 µL) were added to 5 mg of UCNPs modified with alkyne-PEG-neridronate in deionized water with 1 mM KF (0.8 mL). Afterward, the mixture was purged for 45 min with argon, and sodium ascorbate (100 mM, 10 µL) was added to initiate the click reaction. The

dispersion was then purged for another 50 min with argon. To remove the non-bound antibody-azide, the sample was dialyzed in a Float-A-Lyzer G2 dialysis device (300 kDa MWCO) for 72 h against 4 L of dialysis buffer at 4 °C; the buffer was exchanged 9 times. The prepared bioconjugate was stored at 4 °C until further use.

### 1.4 Characterization of the UCNP-based labels

For the transmission electron microscopy (TEM) analysis, a droplet (5 µL) of the UCNP dispersion in cyclohexane was dispersed onto a copper grid covered with a thin layer (12 nm) of carbon foil. The excess dispersion was removed, and the grid was left to dry at room temperature. For imaging the UCNPs on the dried grid, the transmission electron microscope Titan Themis (FEI, Czech Republic) equipped with a Ceta 16-megapixel CMOS camera (FEI, Czech Republic) was used. The particle size was analyzed utilizing the ImageJ software.[6]

To measure the emission spectrum of UCNP-SA bioconjugate under a high excitation intensity utilized during the microfluidic assay, the nanoparticles were immobilized in a submicron layer of agarose.[7] This sample was inserted into the microscope with the camera replaced with a collimator to connect a CCD spectroscope (QE65Pro; Ocean Optics, USA), which recorded the emission spectrum.

Hydrodynamic diameters of the UCNP and MB bioconjugates were analyzed by dynamic light scattering (DLS) utilizing the Zetasizer Nano ZS device (Malvern, UK). The UCNP-SA and UCNP-Ab conjugates were diluted in TBS (150 mM NaCl, 50 mM Tris, 0.05% $NaN_3$, pH 7.5) to 2.5 µg/mL and 1 µg/mL, respectively, and used for the analysis. The MB bioconjugate was diluted in PBS to the concentration of 50 µg/mL. The measurements were carried out at 25 °C in a ZEN0112 plastic cuvette (Malvern, UK).

The concentration and hydrodynamic properties of the UCNP bioconjugates were measured by nanoparticle tracking analysis (NTA) utilizing the NanoSight NS300 device (Malvern, UK). The UCNP-SA and UCNP-Ab conjugates were again diluted in TBS to 2.5 µg/mL and 1 µg/mL, respectively, and used for the analysis. The measurements were carried out utilizing a 532 nm laser source at 25 °C in 5 cycles by 180 s, and the obtained data were normalized.

### 1.5 MTP-based ULISA for the analog detection of PSA

High-binding 96-well microtiter plates (MTPs; Greiner Bio-One, Austria) were used for the reference analog ULISA for PSA. Between the individual assay steps, the MTP was incubated for 1 h at room temperature under shaking at 300 rpm unless stated otherwise. After each step, the wells were washed 4 times with 250 µL of washing buffer.

First, the ab403 anti-PSA monoclonal antibody in coating buffer (100 µL, 1 µg/mL) was incubated in the MTP wells overnight at 4 °C. After blocking with 20% SuperBlock in washing buffer, serial dilutions of PSA ($10^{-4}$ to $10^{2}$ ng/mL) were prepared in 50% serum in assay buffer and added to the MTP wells (100 µL/well). Afterward, BAF1344 biotinylated anti-PSA polyclonal antibody (100 µL, 0.1 and 0.25 µg/mL) was added. Finally, the UCNP-SA bioconjugate (100 µL,

1 and 2 µg/mL) was added. After the last washing step, the MTP was left to dry at room temperature.

### 1.6 Conjugation of MBs with anti-PSA monoclonal antibody

Bioconjugates of MyOne Tosylactivated MBs with the monoclonal anti-PSA antibody (ab403; Abcam, UK) were prepared in accordance with the standard protocol provided by the supplier. For the conjugation reaction, 50 µL of the MB stock solution (100 mg/mL) were utilized. The initial addition of 1 mL of borate buffer (0.1 M $H_3BO_3$, pH 9.5) to the MBs with subsequent mixing of the solution for 30 s and placing it onto a magnetic holder for 3 min was followed by supernatant removal. This step was repeated twice to achieve thorough washing of the MBs. The antibody solution (100 µg of antibody per 5 mg of MBs) was prepared by mixing 19.2 µL of the antibody stock solution (5.2 mg/mL) with 130.8 µL of borate buffer, and the whole volume was added to the MBs. After mixing for 1 min, 100 µL of 3 M ammonium sulfate in phosphate buffer were added, and the resulting mixture was incubated at 37 °C for 18 h under shaking. After 3 min of magnetic separation, the supernatant was removed, followed by the addition of 20% SuperBlock in washing buffer to block the non-specific binding. The mixture was incubated at 37 °C for 1 h under shaking. Afterward, the bioconjugate was washed twice with 1 mL of PBS and resuspended in PBS to a final concentration of 30 mg/mL, considering a 10% loss during the conjugation procedure. The bioconjugate was stored at 4 °C until further use.

### 1.7 Processing of micrographs

ImageJ distribution Fiji[8] was used for visualizing and manual micrograph evaluation. A laboratory-developed software utilizing a convolutional neural network was used for automatic micrograph processing (implemented in Python using the Keras deep learning interface). The micrographs were recorded in 16-bit pixel depth, providing intensity values from ~100 to 65535. Before neural network analysis, these micrographs were logarithmized with a base of two and divided by a factor of 16, resulting in values from ~0.4 to 1.0.

The U-net (**Figure S1**) was selected for its proven capability of localizing diffraction-limited spots. In agreement with previous reports, the model was trained on simulated data.[9] There are two reasons for using simulated data: (i) "ground-truth" data are not easily available for single-particle localization, and (ii) it is possible to simulate realistic images as the physics of imaging single molecules/nanoparticles is well understood.[10]

The spots were simulated as randomly moving two-dimensional Gaussian peaks with a Poisson noise. To introduce a random move, the position of each peak was randomly shifted ten times by a small step (0.1–0.5 µm). Then, the overall shape was integrated over peak positions. To introduce the Poisson noise, the simulated intensity was replaced with a random sample from a Poisson distribution with the mean value equivalent to the simulated intensity. The simulated peaks were superimposed on real micrographs to introduce realistic camera noise and background; the focus in these real images was set slightly above the microfluidic channel, avoiding sharply

focused nanoparticles. A mask indicating the positions of simulated peaks was generated for each training micrograph. The size of simulated micrographs was 256 px × 256 px, 50 peaks were simulated per micrograph, and the training set contained 6000 micrograph-mask pairs with a 25% validation split. Once trained, U-net processed the logarithmized micrographs and returned maps of spot localizations, which were converted to binary masks by thresholding. The binary masks of localizations were used for counting nanoparticles. The U-net processed micrographs of 256 px × 256 px in size. Larger micrographs were processed as fragments of this size, and the counting was made after concatenating the localization masks. Green rectangles marked localized nanoparticles in the overlay with original micrographs to ease manual inspection.

The trained network was tested manually by evaluating real micrographs, and the localization threshold was balanced to limit the number of false-positive and false-negative localizations. The "ground-truth" data were not available to test U-net recognition accuracy. Therefore, the quantitative analysis of recognition accuracy was made by a human expert, manually analyzing 500 images from the real measurement (1024 px × 1024 px; 111 µm × 111 µm) and comparing the results with localization by trained U-net. According to expert estimates, the dataset contained 1979 localizations. The U-net estimated 1883 localizations, which corresponds to 95.1% of those localized by the expert. The rate of false-negative localizations (i.e., spots localized by the expert but not recognized by U-net) was 6.7% (i.e., 132 localizations were missing). The rate of false-positive localizations (i.e., spots localized by U-net but not recognized by the expert) was 1.8% (i.e., 36 false-positive localizations).

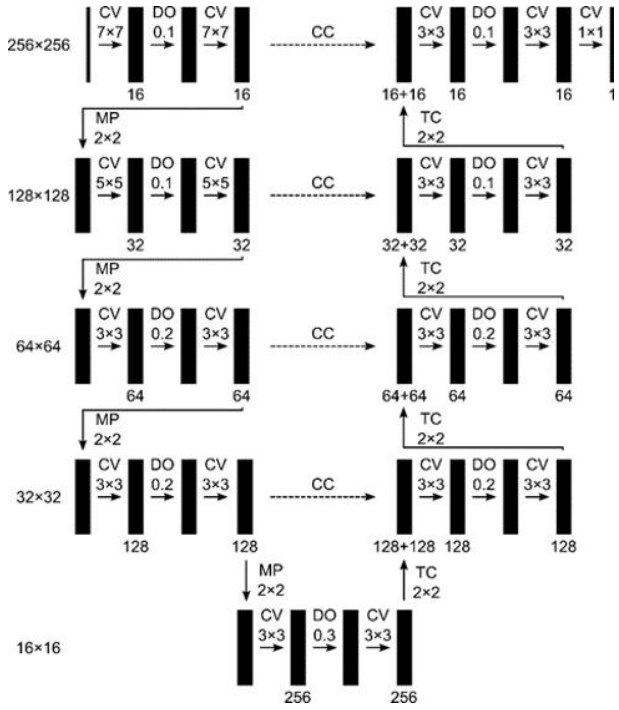


**Figure S1:** Scheme of the utilized U-net. The U-net is composed of convolution (CV), drop out (DO), max pooling (MP), transposed convolution (TC), and concatenation (CC) layers. In the first part, the network successively reduces the size of the input micrograph (256 px × 256 px) to a set of 256 feature maps (16 px × 16 px). In the second part, the map of localizations is built as an output (256 px × 256 px).

### 1.8 Manufacturing the polydimethylsiloxane microfluidic chip

Simple microchannel architecture with a depth of 30 μm and a width of 200 μm was designed in AutoCAD 2015 software (Autodesk, USA) and photolithographically transferred on negative photoresist SU-8 3050 (MicroChem Corp., USA) using a high-resolution laser printer MicroWriter ML3 (Durham Magneto Optics, UK). SYLGARD 184 kit (Dow Corning, USA) was used for polydimethylsiloxane (PDMS) chip fabrication with a 1/10 (w/w) ratio of curing agent, using a standard procedure. The mold was finally bonded upon oxygen plasma treatment to a cover slide with a thickness of 0.17 mm. The thin glass substrate was glued to a protective plastic frame using an epoxy resin to prevent cracks. Silica capillaries with a length of 50 cm and an inner diameter of 50 μm (Molex, USA) were used for connecting the fluid. The ends of capillaries (~1.5 cm length) were tightly fitted with polytetrafluoroethylene tubes, which served as robust connectors for the PDMS chip (1/16" outer diameter and 0.01" inner diameter; Alltech, Czech Republic).

## 2 Results and discussion

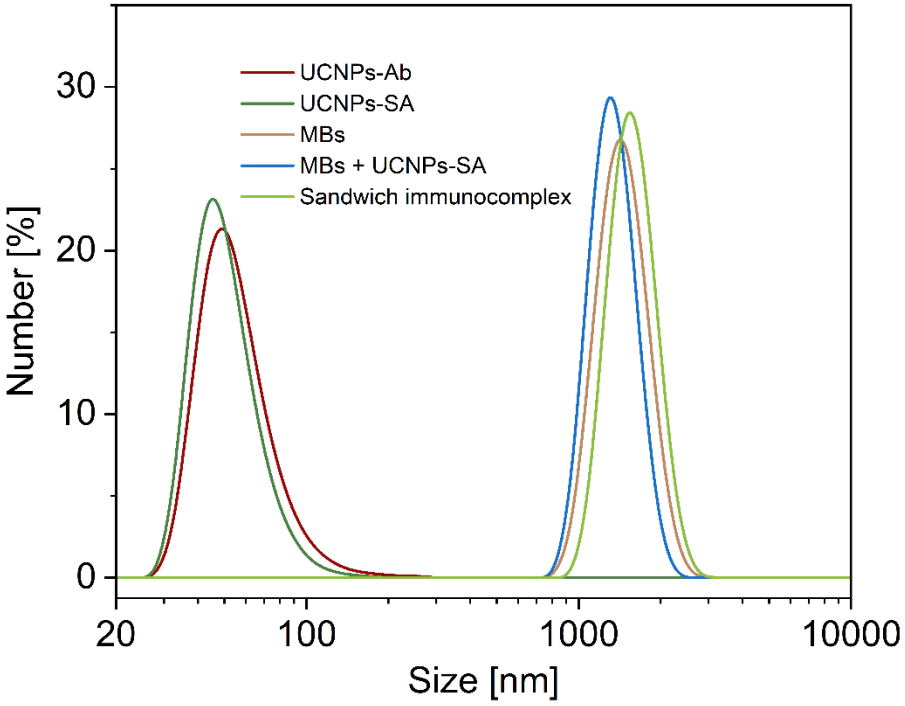


**Figure S2**: DLS characterization of the UCNP-Ab and the UCNP-SA bioconjugates, as well as the MB bioconjugates under various conditions (unbound MBs, MBs mixed with the UCNP-SA, and MBs after the immunocomplex formation). The distribution is based on the number of MBs; the data points were connected using a B-spline function.

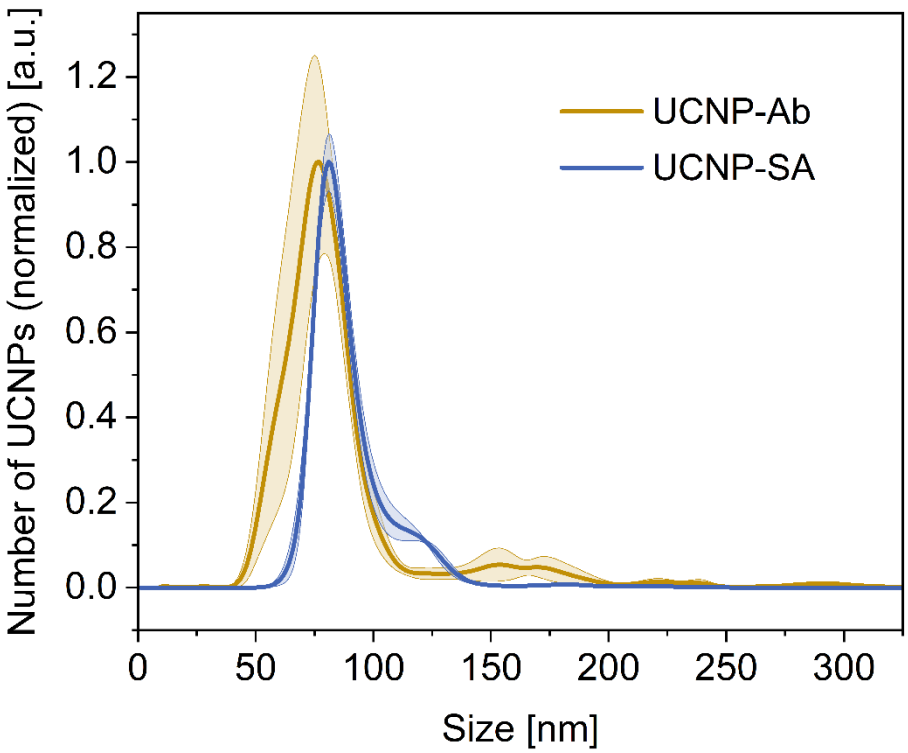


**Figure S3:** Nanoparticle size distribution obtained from the NTA measurement of the UCNP-Ab and UCNP-SA bioconjugates. The bands around the curves represent the standard deviations. For the UCNP-SA, the most represented nanoparticle size was 89.8 ± 0.5 nm, with the calculated stock concentration of $9.1\times10^{11}$ particles/mL. For the UCNP-Ab, the size was 92.9 ± 5.4 nm, with a stock concentration of $8.2\times10^{10}$ particles/mL. The UCNP-Ab displayed a wider distribution of sizes, as well as a small number of aggregates, confirming the results of the DLS analysis.

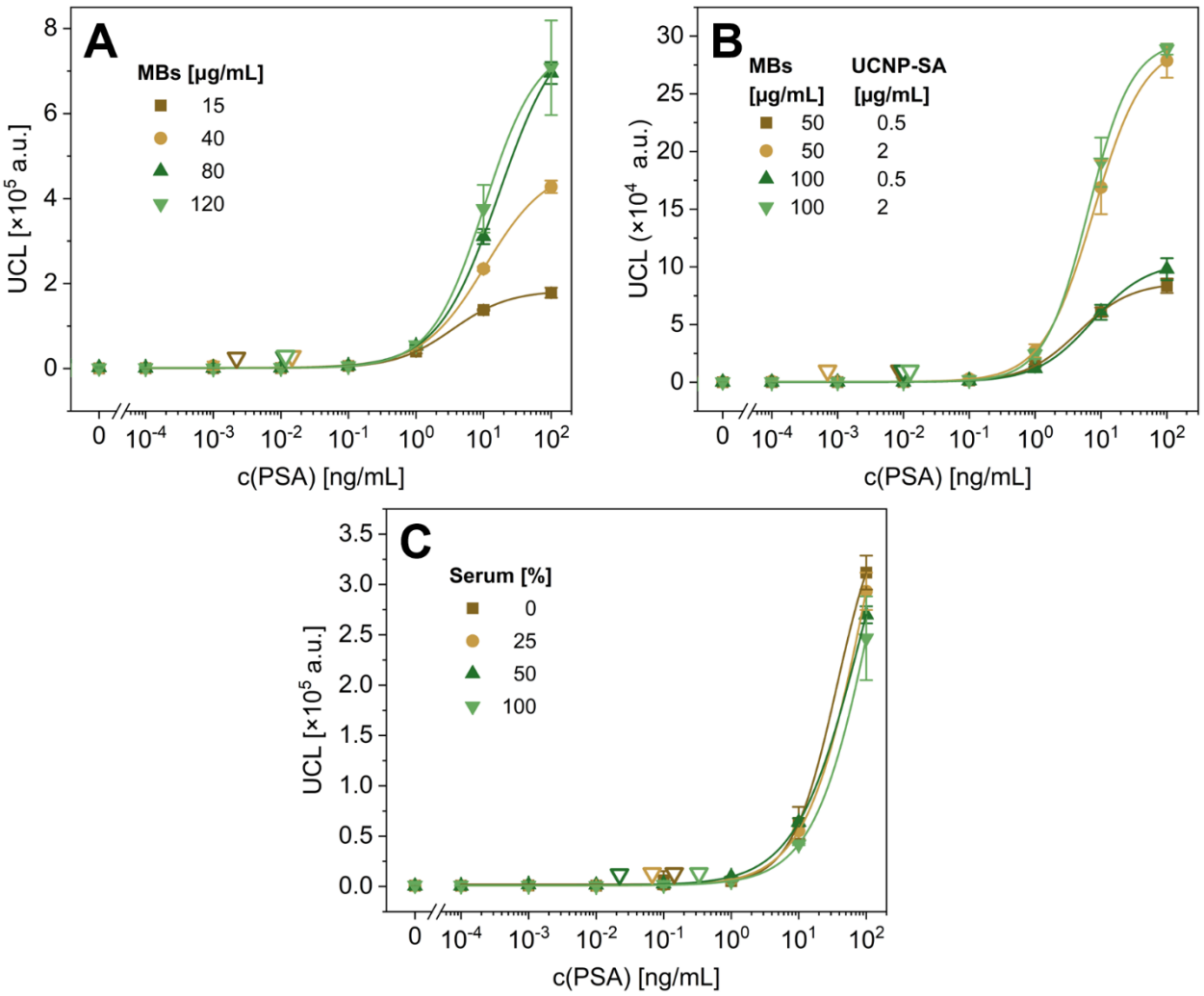


**Figure S4:** Optimization of the MB-based ULISA for the PSA detection. (**A**) Optimization of MB concentration; the assay showed the optimal performance was achieved with the MB bioconjugate at 80 µg/mL (LOD of 11.5 pg/mL). (**B**) Optimization of the ratio of MBs and UCNPs; the best results were achieved with MBs in the concentration of 50 µg/mL combined with a UCNP-SA concentration of 2 µg/mL (LOD of 0.7 pg/mL). (**C**) Testing the effect of fetal bovine serum concentration on the assay performance; the results showed that the use of serum did not significantly affect the assay performance. The empty triangles represent the LODs, and the error bars represent standard deviations from three independent wells.

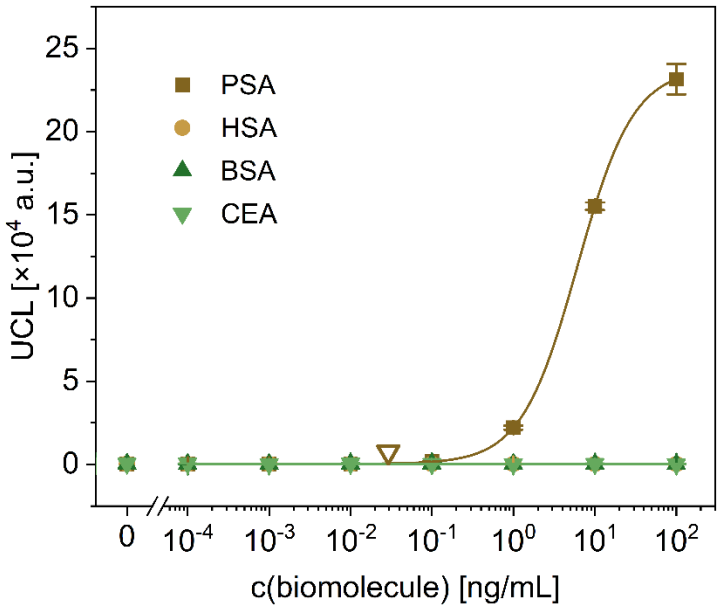


**Figure S5:** MB-based ULISA for the detection of PSA, with human serum albumin (HSA), bovine serum albumin (BSA), and carcinoembryonic antigen (CEA) used to verify the assay specificity. The empty triangle represents the LOD, and the error bars represent the standard deviations of three measurements.

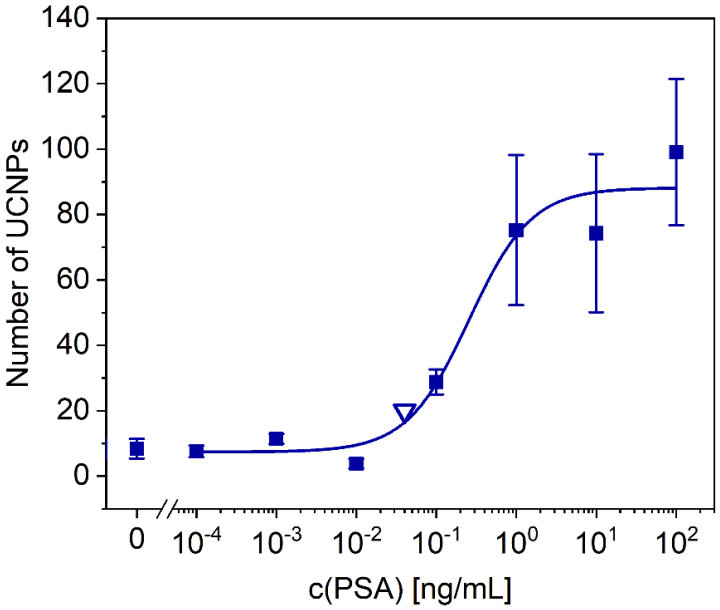


**Figure S6:** Optimization of the digital MB-based ULISA in the microfluidic device for PSA detection using a 50-µm capillary, MB concentration of 50 µg/mL, and the UCNP-SA concentration of 2 µg/mL. The empty triangle represents the LOD, and the error bars represent the standard deviations of three measurements.

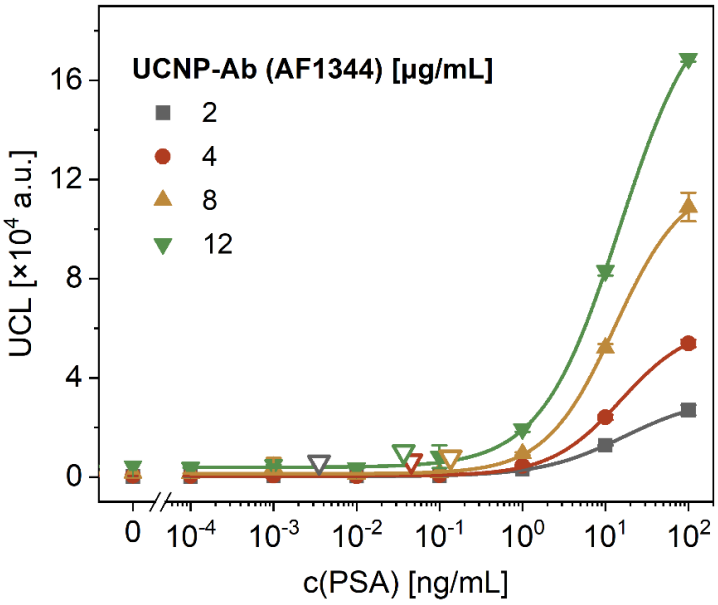


**Figure S7:** Optimization of the UCNP-Ab bioconjugate concentration in MTP-based ULISA for the detection of PSA. The empty triangles represent the LODs, and the error bars represent the standard deviations of three wells.

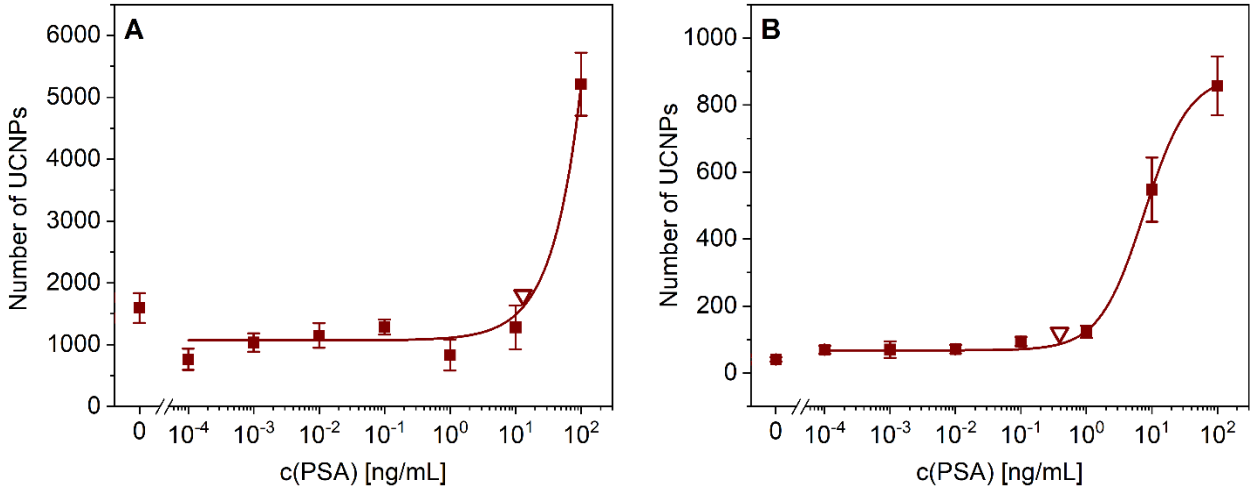


**Figure S8:** Optimization of the digital MB-based ULISA in the microfluidic device for PSA detection using the UCNP-Ab bioconjugate in the concentration of (**A**) 12 µg/mL and (**B**) 4 µg/mL. The empty triangles represent the LODs, and the error bars represent the standard deviations of three measurements.

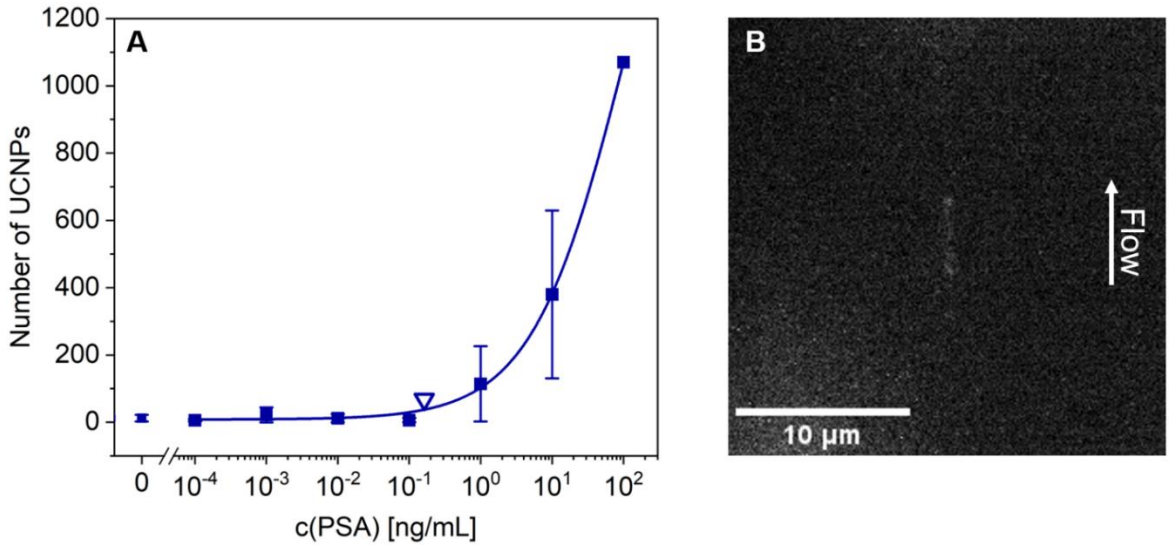


**Figure S9:** (**A**) Optimization of the digital MB-based ULISA in the microfluidic device for PSA detection with more intense mixing, using the MB concentration of 50 µg/mL and the UCNP-SA concentration of 2 µg/mL. The empty triangle represents the LOD, and the error bars represent the standard deviations of three measurements. (**B**) A single UCNP moving through the flow-through cell at high speed, appearing as an elongated line.

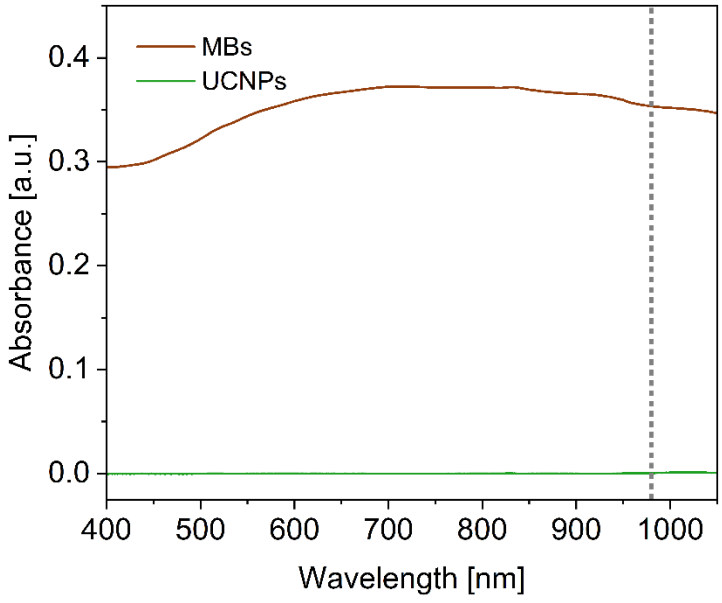


**Figure S10:** The absorption spectra of the MB-ab403 (50 µg/mL) and UCNP-SA (2 µg/mL) bioconjugates. The spectra were evaluated at the wavelength of 980 nm (highlighted with the dotted line), which was used for the excitation of UCNPs in the microfluidics measurements.

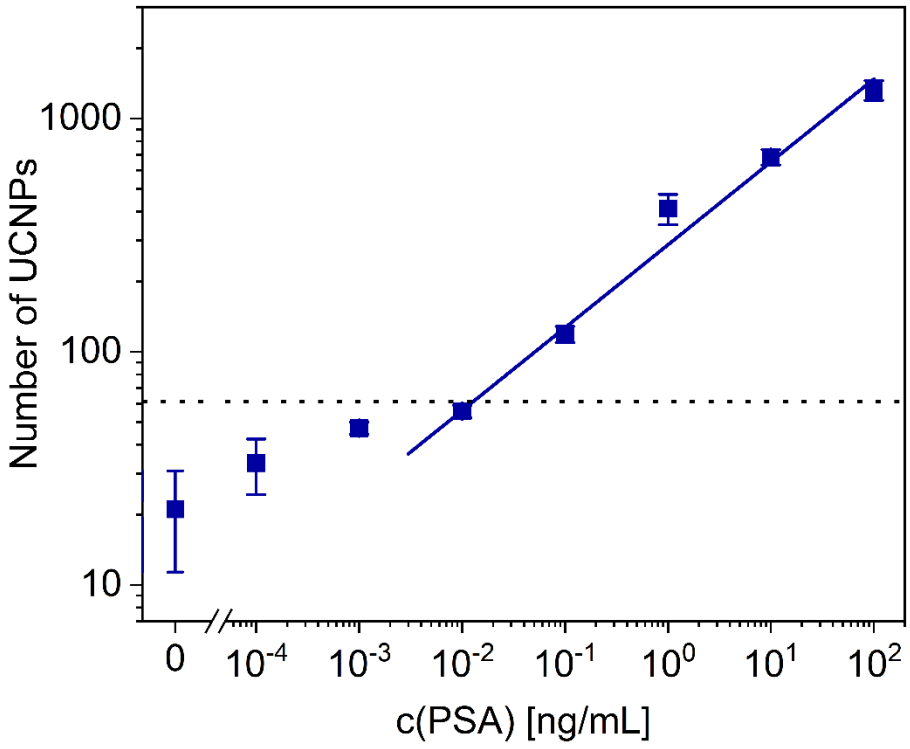


**Figure S11**: The results of optimized in-flow digital readout of the MB-based ULISA for the detection of PSA plotted in a double logarithmic scale and fitted utilizing a linear function. The LOD was calculated as an intersection of the linear part of the calibration with the sum of the blank and the treble of the standard deviation of the blank. This LOD has reached the value of 12 pg/mL, which is 11.5 times higher than the one calculated *via* the 4-parameter logistic fit.

**Table S1:** Precision of the microfluidic measurement. The experimental coefficients of variation (CVs) were calculated by dividing the standard deviation of three measurements by the average number of UCNPs per measurement. The Poisson noise was calculated by dividing the square root of the average number of UCNPs per experiment (using the imaging area of 111 µm × 111 µm in the sample plane) by the average number of UCNPs ($\sqrt{n}/n$).

| PSA [ng/mL] | Average number of UCNPs | Experimental CV [%] | Poisson noise [%] |
|---|---|---|---|
| 0 | 21.1 ± 9.8 | 46.3 | 21.9 |
| $10^{-4}$ | 33.3 ± 8.9 | 26.6 | 17.3 |
| $10^{-3}$ | 47.1 ± 2.9 | 6.1 | 14.5 |
| $10^{-2}$ | 55.6 ± 3.5 | 6.2 | 13.4 |
| $10^{-1}$ | 118.9 ± 9.5 | 7.9 | 9.2 |
| 1 | 411.3 ± 61.3 | 14.9 | 4.9 |
| 10 | 684 ± 52 | 7.6 | 3.8 |
| $10^{2}$ | 1326 ± 128 | 9.7 | 2.7 |

**Table S2:** Detection of PSA in clinical samples of human serum utilizing the upconversion scanner and the microfluidic device for the readout of MB-based ULISA. The reference values were obtained by the Elecsys electrochemiluminescence immunoassay analyzer (Roche Diagnostics, Germany). The averages and standard deviations were calculated from three wells, and three measurements, respectively.

| Reference [ng/mL] | Analog readout | | | | Digital readout | | | |
|---|---|---|---|---|---|---|---|---|
| | Dil. | Found (diluted) [ng/mL] | Found (original) [ng/mL] | Recovery rate [%] | Dil. | Found (diluted) [ng/mL] | Found (original) [ng/mL] | Recovery rate [%] |
| 2.08 | 10× | 0.182 ± 0.003 | 1.82 ± 0.03 | 87.8 ± 1.6 | 4× | 0.51 ± 0.18 | 2.0 ± 0.7 | 97 ± 33 |
| 9.23 | 10× | 1.00 ± 0.03 | 10.0 ± 0.3 | 108.5 ± 2.8 | 10× | 0.89 ± 0.06 | 8.9 ± 0.6 | 97 ± 6 |
| 30.64 | 100× | 0.341 ± 0.016 | 34.1 ± 1.6 | 111 ± 5 | 10× | 3.2 ± 0.6 | 32 ± 6 | 105 ± 20 |

# 3 References


1 V. Poláchová, M. Pastucha, Z. Mikušová, M. J. Mickert, A. Hlaváček, H. H. Gorris, P. Skládal and Z. Farka, *Nanoscale*, 2019, **11**, 8343–8351.

2 A. Hlaváček, Z. Farka, M. J. Mickert, U. Kostiv, J. C. Brandmeier, D. Horák, P. Skládal, F. Foret and H. H. Gorris, *Nat. Protoc.*, 2022, **17**, 1028–1072.

3 J. C. Brandmeier, K. Raiko, Z. Farka, R. Peltomaa, M. J. Mickert, A. Hlaváček, P. Skládal, T. Soukka and H. H. Gorris, *Adv. Healthc. Mater.*, 2021, **10**, 2100506.

4 J. C. Brandmeier, N. Jurga, T. Grzyb, A. Hlaváček, R. Obořilová, P. Skládal, Z. Farka and H. H. Gorris, *Anal. Chem.*, 2023, **95**, 4753–4759.

5 E. Makhneva, D. Sklenárová, J. C. Brandmeier, A. Hlaváček, H. H. Gorris, P. Skládal and Z. Farka, *Anal. Chem.*, 2022, **94**, 16376–16383.

6 C. A. Schneider, W. S. Rasband and K. W. Eliceiri, *Nat. Methods*, 2012, **9**, 671–675.

7 A. Hlaváček, J. Křivánková, H. Brožková, J. Weisová, N. Pizúrová and F. Foret, *Anal. Chem.*, 2022, **94**, 14340–14348.

8 J. Schindelin, I. Arganda-Carreras, E. Frise, V. Kaynig, M. Longair, T. Pietzsch, S. Preibisch, C. Rueden, S. Saalfeld, B. Schmid, J.-Y. Tinevez, D. J. White, V. Hartenstein, K. Eliceiri, P. Tomancak and A. Cardona, *Nat. Methods*, 2012, **9**, 676–682.

9 A. Speiser, L.-R. Müller, P. Hoess, U. Matti, C. J. Obara, W. R. Legant, A. Kreshuk, J. H. Macke, J. Ries and S. C. Turaga, *Nat. Methods*, 2021, **18**, 1082–1090.

10 L. Möckl, A. R. Roy and W. E. Moerner, *Biomed. Opt. Express*, 2020, **11**, 1633–1661.